# Towards Scalable Exact Machine Unlearning Using Parameter-Efficient Fine-Tuning

Somnath Basu Roy Chowdhury<sup>1</sup>, Krzysztof Choromanski<sup>2, 3</sup>, Arijit Sehanobish<sup>4</sup>, Avinava Dubey<sup>5</sup>, Snigdha Chaturvedi<sup>1</sup>

<sup>1</sup>UNC Chapel Hill, <sup>2</sup>Google DeepMind, <sup>3</sup>Columbia University, <sup>4</sup>Independent, <sup>5</sup>Google Research. {somnath, snigdha}@cs.unc.edu

## **Abstract**

Machine unlearning is the process of efficiently removing the influence of a training data instance from a trained machine learning model without retraining it from scratch. A popular subclass of unlearning approaches is exact machine unlearning, which focuses on techniques that explicitly guarantee the removal of the influence of a data instance from a model. Exact unlearning approaches use a machine learning model in which individual components are trained on disjoint subsets of the data. During deletion, exact unlearning approaches only retrain the affected components rather than the entire model. While existing approaches reduce retraining costs, it can still be expensive for an organization to retrain a model component as it requires halting a system in production, which leads to service failure and adversely impacts customers. To address these challenges, we introduce an exact unlearning framework – Sequence-aware Sharded Sliced Training (S<sup>3</sup>T), which is designed to enhance the deletion capabilities of an exact unlearning system while minimizing the impact on model's performance. At the core of S<sup>3</sup>T, we utilize a lightweight parameter-efficient fine-tuning approach that enables parameter isolation by sequentially training layers with disjoint data slices. This enables efficient unlearning by simply deactivating the layers affected by data deletion. Furthermore, to reduce the retraining cost and improve model performance, we train the model on multiple data sequences, which allows S<sup>3</sup>T to handle an increased number of deletion requests. Both theoretically and empirically, we demonstrate that S<sup>3</sup>T attains superior deletion capabilities and enhanced performance compared to baselines across a wide range of settings.

# 1 Introduction

In recent years, the growing success of machine learning (ML) has led to its widespread deployment across a range of applications [1, 58, 49]. Once a machine learning model has been trained, it may be necessary to *unlearn* specific training data instances for various reasons, like complying with user data deletion requests [43, 18, 52, 2], removing stale or corrupt data [5, 53], etc. Retraining an ML model entirely from scratch with each deletion request is expensive, especially for modern large-scale models [9, 1, 58]. Machine unlearning [46, 65] techniques focus on efficiently unlearning the influence of a data instance from a trained ML model.

Machine unlearning techniques can be classified into two broad categories: approximate and exact unlearning. Approximate unlearning techniques [26, 40] modify the parameters of a trained model to reduce the influence of the deleted data instance. While cost-effective in practice, approximate unlearning cannot guarantee the complete removal of an instance's influence and it may still retain

<sup>&</sup>lt;sup>1</sup>Work in Progress.

non-zero influence on the model. Moreover, auditing approximate unlearning is challenging due to the stochastic nature of ML optimization [59]. An alternative to this approach is exact unlearning [10, 8], which can guarantee the removal of the influence of a data instance from a trained model. Exact unlearning techniques use a modular system, where different components within the system are trained on disjoint subsets of the data. When a deletion request occurs, only the affected component needs to be retrained. However, in real-world settings, halting a production system to even retrain a single component can result in service failure and significant expenses for a business. The alternative is to function without the affected component, which may result in reduced performance, ultimately impacting end users. To address these challenges, we introduce an efficient exact unlearning framework, Sequence-aware Sharded Sliced Training (S³T), which enhances the system's deletion capability while minimizing the impact on performance.

The key idea behind our S³T framework is to perform additional offline training before deploying the initial model to reduce retraining costs. At the core of S³T, we leverage a novel lightweight parameter-efficient fine-tuning (PEFT) that allows parameter isolation by sequentially training model layers using disjoint data slices. Due to this parameter isolation, it is possible to efficiently perform exact unlearning by deactivating the layers associated with the deleted instance, rather than discarding the entire checkpoint. We efficiently train multiple models using different sequences of the same data slices. We show that increasing the training budget before deployment can significantly reduce retraining costs and improve the model's performance in production. We also observe that it is important to train the model using diverse sequences and provide an optimal algorithm for selecting such sequences using graph matching [13]. Furthermore, we formalize the notion of deletion rate for exact unlearning systems and theoretically show that S³T achieves provably better deletion guarantees than existing approaches. We conduct extensive empirical evaluations to evaluate the effectiveness of our proposed fine-tuning approach using Transformers with parameter counts ranging from 86M to 13B on a range of tasks. Additionally, we empirically validate the sequence selection algorithm and show that S³T has superior deletion performance compared to existing methods.

The rest of the paper is organized as follows: (a) We introduce the prior literature related to approximate and exact machine unlearning (Section 2), (b) We describe the problem setup for exact unlearning (Section 3.1), (c) We introduce the fine-tuning approach, S<sup>3</sup>T, and sequence selection algorithm under budget constraints (Section 3.2 & 3.3), (d) We theoretically analyze several properties of S<sup>3</sup>T (Section 3.4), and (e) We present experiments to evaluate the effectiveness of S<sup>3</sup>T's fine-tuning approach, deletion performance and sequence selection algorithm (Section 4).

## 2 Background

Machine unlearning techniques [10] for deep learning can be broadly classified into two categories: *approximate* and *exact* unlearning. Approximate unlearning techniques focus on reducing the influence of a deleted instance from a model after it has been trained. Exact unlearning techniques provide unlearning guarantees by ensuring learning components trained on a deleted instance are not used during inference. In this section, we discuss each of these categories in detail.

**Approximate Machine Unlearning**. These techniques focus on approximating the model parameters as if the deleted data instance was not there in the training set from the beginning [26]. These techniques typically quantify the influence of an instance [33] and perform gradient ascent for unlearning [22, 23, 45, 51, 27, 54, 40]. In contrast to these approaches, [25] stores the exact gradients encountered during training and uses them directly for gradient ascent. Another line of work [56, 57, 32, 11, 17, 48, 36, 41] focuses on unlearning in a batch setting, where they assume access to both a retention set and a forgetting set of data instances for approximate unlearning. While efficient in practice, auditing approximate unlearning techniques is challenging due to the stochastic nature of the optimization process [59, 63] and may have weak privacy guarantees in practice [28].

**Exact Machine Unlearning.** These techniques focus on developing a modular machine learning system, where individual components are trained using disjoint subsets of the data. Such a system offers the advantage that when a deletion request is received for an input instance, we only need to retrain the affected component rather than the entire model. The first instance of such a modular system: Sharded, Isolated, Sliced, and Aggregated training (SISA) [8]. SISA uses an ensemble of models each trained on a disjoint shard of the dataset as shown in Figure 1 (left). To further reduce retraining costs, each shard is divided into slices, and the models are incrementally trained on these slices, with their checkpoints stored sequentially (shown in Figure 1 (right)). If a deletion request is

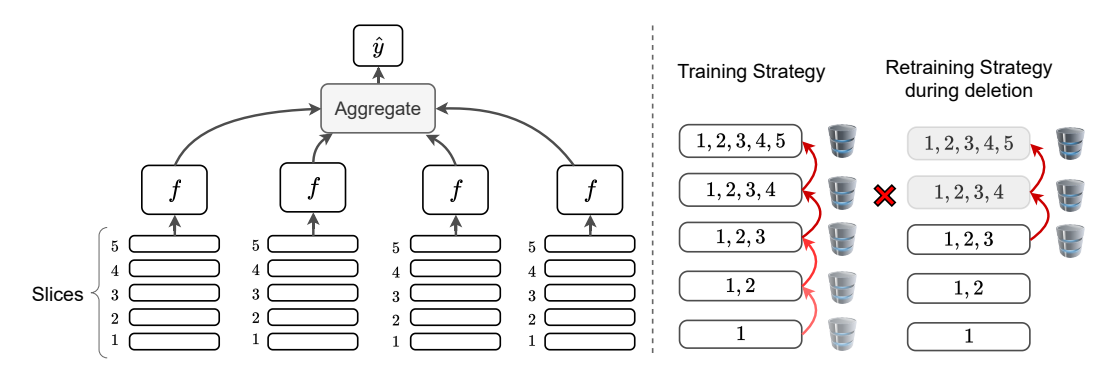


Figure 1: Schematic diagram of the Sharded, Isolated, Sliced, and Aggregated training (SISA) [8] framework. An ensemble of models is individually trained on disjoint shards. (*Left*) Each shard is further divided into slices. (*Right*) Each model is sequentially trained on the slices and checkpoints are stored. After deletion, retraining resumes from the best available checkpoint.

received for a data instance within 4<sup>th</sup> slice of a shard, we must retrieve the checkpoint from the 3<sup>rd</sup> slice and retrain using the remaining data within that shard. Several approaches focus on improving the components within SISA in application-specific settings like enhancing the dataset partitioning mechanism [3, 66], the retraining efficiency using light-weight adapters [35, 16], or extending the modular approach for vision tasks by using compartmentalized diffusion models [24]. However, these approaches are orthogonal to our work since they do not fundamentally modify the functioning of SISA and therefore can be easily incorporated within our proposed framework.

SISA is a well-known framework that can guarantee exact unlearning and has found widespread applications. However, using SISA within production systems is challenging because retraining even a single component would result in downtime, thereby reducing the service level agreement (SLA). Furthermore, in the worst-case scenario, if deletion requests impact the first slice in all the shards, the entire service goes down, necessitating retraining the model from scratch. In this work, we leverage parameter-efficient fine-tuning to introduce a framework that improves upon the service availability and deletion capabilities of the SISA framework.

# 3 Sequence-aware Sharded Sliced Training (S<sup>3</sup>T)

In this section, we describe the functioning of our proposed exact unlearning framework, Sequence-aware Sharded Sliced Training (S<sup>3</sup>T). This framework leverages parameter-efficient fine-tuning (PEFT) to build an exact unlearning framework.

## 3.1 Problem Setting

We consider the general setting where the user fine-tunes a pre-trained model [14, 60] on private data using PEFT techniques. We assume that the deletion requests affect only the private fine-tuning data, not the pre-training data. Our framework, S³T, uses a setup where the dataset is divided into disjoint shards, with each shard further divided into slices. In S³T, we partition a dataset  $\mathcal{D} = \{\mathcal{D}_1, \dots, \mathcal{D}_m\}$  into m disjoint shards. Each shard is further divided into L slices:  $\mathcal{D}_i = \{S_1, \dots, S_L\}$ . S³T trains a separate model for each shard and uses their aggregate decision.

Existing unlearning frameworks SISA [8] use a similar setup described above. In SISA, within each shard, the model is trained in multiple stages sequentially on the slices (training stages are Slice 1, Slice 1+2, and so on), and their checkpoints are stored. However, a key weakness of SISA is that individual models within the ensemble need to be retrained whenever a deletion request is executed. Even retraining on a single slice is expensive for large-scale models in production serving a huge customer base. A naive alternative would be to use the last known usable checkpoint and perform retraining after regular intervals. For example, in Figure 1 (right), if a deletion request arrives for a data instance in Slice 3, the model in production can be replaced with the checkpoint obtained after Slice 2. It is easy to see that the performance of the overall model will degrade with the number of deletion requests. In the extreme scenario where deletion requests target Slice 1 of all shards, the entire service goes down necessitating retraining from scratch.

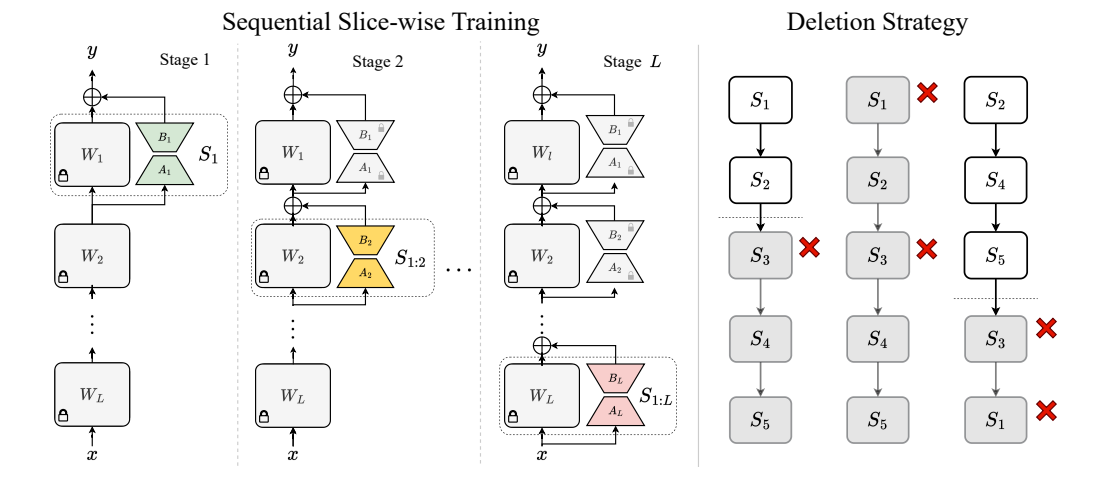


Figure 2: (Left) We show the schematic diagram of the slice-wise training strategy in  $S^3T$ . We incrementally train the model  $-i^{th}$  layer (from the top) using slices  $S_{1:i}$  while keeping the other layers fixed. (Right) We show the impact of deletion on models trained on different permutations of slices.

We present an exact unlearning framework, S<sup>3</sup>T, to address these challenges. The core idea involves training several copies of the model with different slice sequences. When deletion requests occur, we utilize the model trained on a sequence that minimizes performance degradation. To further reduce the training cost, we leverage PEFT techniques and present a novel sequential slice-wise fine-tuning strategy in Section 3.2. Our training strategy allows us to use the same model by deactivating certain layers without the need to swap checkpoints in case of a deletion. In the following sections, we introduce the fine-tuning strategy and demonstrate how to select diverse data sequences for training.

## 3.2 Sequential Slice-wise Training

In this section, we introduce Sequence-aware Sharded Sliced Training (S³T) a lightweight fine-tuning approach using parameter-efficient fine-tuning (PEFT) for efficient exact unlearning. This fine-tuning approach enables parameter isolation by sequentially training PEFT layers using different data slices. Due to this parameter isolation, it is possible to efficiently handle deletion requests by deactivating layers associated with the instance.

We describe our approach using the PEFT technique, LoRA [31], but our method is general can be easily extended to other PEFT techniques. LoRA introduces a small number of trainable low-rank  $(r \ll d)$  parameters,  $(\mathbf{X}, \mathbf{Y})$ , while the pre-trained weights  $\overline{\mathbf{W}}$  remains fixed as shown below:

$$\mathbf{W} = \overline{\mathbf{W}} + \mathbf{X}^{\mathsf{T}} \mathbf{Y}, \text{ where } \mathbf{X}, \mathbf{Y} \in \mathbb{R}^{r \times d}, \overline{\mathbf{W}} \in \mathbb{R}^{d \times d}.$$
 (1)

Our key idea involves training different LoRA layers using different slices of data. This approach allows us to selectively deactivate (zero out) the LoRA parameters ( $\mathbf{X}$  or  $\mathbf{Y}$ ) associated with a particular layer in the event of data deletion from that slice. In Figure 2 (left), we illustrate the training process in detail, where we follow a sequential top-to-bottom training approach. At stage 1, we train the final layer of the model (Layer 1 in the Figure) using data slice 1 while LoRA parameters from all other layers are switched off. In the next stage, we train Layer 2 using data slices 1 and 2, while keeping the LoRA parameters from the 1<sup>st</sup> layer frozen. This process continues for the rest of the layers. Note that our training process does not need to proceed in a layer-wise fashion, where each layer is trained on a different data slice. The user can even train k-LoRA layers per data slice resulting in a total of kL layers being trained.

The sequential slice-wise training process ensures that the LoRA parameter updates at the i-th layer are a function of the data instances within slices  $\{1,\ldots,i\}$ . Therefore, if a deletion request affects the i-th slice, the same model can still be used by deactivating the LoRA parameters corresponding to slices  $\{i,\ldots,L\}$  (see details in Algorithm 3). For example, if a deletion request affects slice  $S_3$  only the subsequent LoRA layers need to be deactivated to ensure exact unlearning, as shown in the first example of Figure 2 (right). This is because during training the parameters of layers 1 & 2 were not affected by instances in  $S_3$ . Now consider the scenario where deletion requests affect multiple

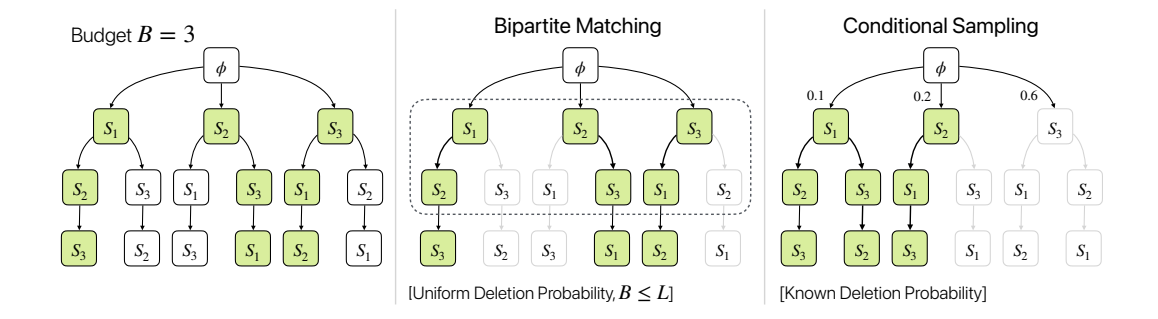


Figure 3: Illustration of the slice sequence selection problem under a budget constraint. (Left) An example of a permutation tree with L=3 and a diverse set of sequences for budget B=3 is shown in green. (Center) We show the intuition behind the BMS algorithm, where a bipartite graph is formed between successive layers, and we find a perfect matching between them. (Right) Illustration of the conditional sampling, where each slice is selected sequentially based on the deletion probabilities.

slices. This is shown in the second example of Figure 2 (right), where slices  $S_1$  and  $S_3$  are affected. In this case, we observe that a model trained on the default ordering of the sequence  $\{S_1,\ldots,S_L\}$  is rendered useless when  $S_1$  and  $S_3$  are affected. This motivates us to train multiple models using different permutations of the slices. This would enhance the service time and system performance by selecting a model trained with the most effective ordering (e.g., the third ordering in Figure 2 (right) yields the best-performing model). However, training on all permutations of slices, L!, is expensive. In the following section 3.3, we present an algorithm to select a diverse set of permutations under resource constraints.

**Design Choices**. Here, we discuss the rationale behind the design choices for the proposed slice-wise training approach. First, we use top-to-bottom fine-tuning because we found the top layers were easier to train at the start and a bottom-up approach didn't converge. Second, we train layers in a cumulative manner where the i-th layer is trained using slices  $\{1,\ldots,i\}$ . We found that this way of training helps in better convergence compared to the setup where we train every layer using a different slice. Third, we analyze the cost of slice-wise training and find it to be comparable to full training. Considering that training cost is c = O(nl), where n is the dataset size and l is the number of trainable layers (empirical evidence in Appendix C.2). For slice-wise training, we observe that  $c = \sum_{i=1}^k \left(\frac{in}{k}\right) \left(\frac{l}{k}\right) = O\left(\frac{nl}{2}\right)$ , which is of the same order as full training.

#### 3.3 Training under Budget Constraints

The training strategy discussed in the previous section requires training the same model on L! slice sequences, which is expensive in practice. In this section, we discuss strategies to select sequences under a budget, B (maximum number of sequences that can trained). First, we show that there exists an optimal subset of B slice sequences and randomly selecting B sequences may not be effective. To illustrate this idea, we use a permutation tree [4], where all possible permutation sequences are embedded into a tree structure. In Figure 3 (left), we show an example of a permutation tree with L=3 slices, paths from the root to the leaves correspond to unique slice sequences  $(S_1,S_2,S_3)$ ,  $(S_1, S_3, S_2)$ , and so on. From the previous section, we know that the topmost slice is most sensitive because if a deletion request affects the topmost slice the entire model needs to be retrained (shown in Figure 2 (right)). To address this and reduce the retraining cost, we should ensure we train models on sequences with different top slices. Building on this intuition, in the general setting we should train the model on diverse permutation sequences. An example is illustrated in Figure 3 (left), where a diverse set of 3 sequences is marked in green (where no identical slices occupy the same position). Selecting diverse permutations is challenging for two reasons: (a) relying solely on random sampling may not always yield optimal results, and (b) performing naive random sampling may not be feasible with large slice counts, e.g., L=32, where even enumerating all 32! permutations becomes prohibitively expensive. Next, we provide two strategies to select permutation sequences for a budget B.

Uniform Deletion Prior, Budget  $B \leq L$ . The first strategy is called Bipartite-matching based Selection (BMS), which is designed for the setting where budget  $B \leq L$  and each slice has a uniform probability of being impacted by deletion. This scenario is quite common when the budget is limited

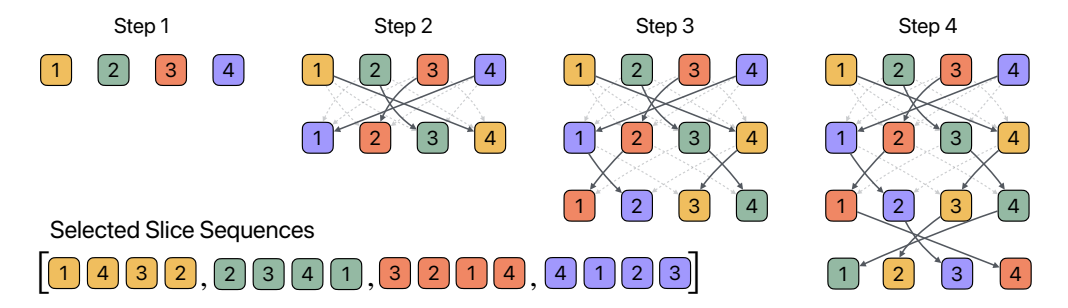


Figure 4: We show the functioning of the BMS algorithm for L=4 slices, B=4. BMS selects one element in each permutation sequence at a time. This is performed by constructing a bipartite graph with all feasible edges to the next node and selecting a matching with the previously selected set. The dark gray arrows  $(\rightarrow)$  indicate the selected edges and dotted arrows  $(-\rightarrow)$  the feasible ones.

and deletion probabilities for slices are unknown. In this setting, finding the most diverse permutation set can be decomposed into solving the perfect matching in bipartite graphs [21]. We describe the intuition behind BMS using a permutation tree in Figure 3 (center), wherein we sequentially select elements of the permutations. The exact functioning of BMS is shown in Figure 4. BMS iteratively selects elements of sequences by defining a bipartite graph between one level to the next one using the edges of the permutation tree (where edges are incident on feasible elements that haven't been encountered in the sequence). Selecting the next element then is equivalent to finding a perfect matching [19] between one level and the next one as shown by the bold lines in Figure 4. This continues till all sequences have L elements. Overall, BMS has a time complexity of  $O(L^{2.5})$  (details in Appendix B.1). The following result shows that BMS is optimal (proof in Appendix A.1).

**Lemma 1.** For a budget  $B \leq L$ , BMS returns the most diverse set of B permutations.

Known Deletion Prior. The next strategy addresses the general case where B can be anything and assume access to deletion probabilities for each slice. For simplicity, we consider the probability of a deletion request affecting a slice as  $\{p_1,\ldots,p_L\}$ . The intuition behind this approach is to ensure that slices with a lower probability of deletion are placed at the start of the sequence. Therefore, we use a conditional sampling strategy to construct individual sequences by sampling one slice at a time according to the probability of not being deleted  $(1-p_i)$ . This process is shown in Figure 3 (right), where we select the next slice in a sequence. We repeat this sampling process till we have B unique sequences and use them for training. We can use the same algorithm when deletion priors are unknown by considering a uniform distribution. Note that conditional sampling may not return the optimal permutation subset and has similar guarantees as random sampling but without its computational bottleneck. Selecting the B most diverse permutations is a challenging combinatorial problem, which to the best of our knowledge, has not been extensively studied in the algorithms literature. We defer the task of developing a general algorithm for this problem to future works.

#### 3.4 Theoretical Analysis

In this section, we theoretically analyze the performance of exact unlearning system. For this, we draw inspiration from approximate unlearning literature [51] and introduce the definition of *deletion rate* for exact unlearning systems.

**Definition 1** (Deletion Rate). The deletion rate,  $\delta(S)$ , of an exact unlearning system S, is the expected number of deletion requests until the system needs to be retrained from scratch.

The deletion rate captures the effectiveness of an exact unlearning system by quantifying the expected number of deletion requests it can handle. Next, we theoretically quantify the deletion rate for S<sup>3</sup>T and compare it with that of SISA.

**Lemma 2.** For  $B \ge L$  and dataset size  $N \gg r$ , where r is the number of deletion requests, the deletion rate of  $S^3T$  is  $\delta(S^3T) \sim O(mL\log(mL))$  and for SISA it is  $\delta(\operatorname{SISA}) \sim O(mL\log m)$ , where m is the number of shards and L is the number of slices per shard.

The proof is presented in Appendix A.2. The above result is based on the simple observation that when the budget  $B \ge L$ , deletion requests should impact all mL slices (m: number of shards, L: slices per shard) across shards for S<sup>3</sup>T to encounter service failure. However, in the case of SISA, if

deletion requests affect the first slice of every shard (total of m slices), then the system will experience service failure and need to be retrained from scratch.

Next, we analyze the impact of deletion requests on the system's performance. We perform a fine-grained analysis focusing on an individual shard performance. In this setting, we consider the real-world scenario where we do not retrain every time a slice is impacted instead work with the best available model. For S³T, this means switching off the necessary PEFT layers, while for SISA, it means reverting to the best available checkpoint. The unlearning system experiences performance degradation with an increasing number of deletion requests, as we are compelled to utilize a model trained on fewer data slices (we show this empirically in Section 4.2). To quantify the performance retention we use a monotonically increasing function F(k), which indicates a model's performance when trained on k slices. The exact formulation of  $F(\cdot)$  depends on several factors like the dataset, model size, etc. We analyze the performance retention while processing deletion requests.

**Lemma 3** (Performance Retention). Given a budget B, the probability that a shard retains a performance,  $F_r(\cdot)$ , of at least F(k) after r deletion requests is shown below

$$\mathbb{P}\left[F_r(\mathcal{S}^{\mathfrak{I}}\mathcal{T}) \geq F(k)\right] = B'\left(1 - \frac{k}{L}\right)^r, \text{ where } B' = \min\left\{B, \binom{L}{k}\right\}, k \in [1, \dots, L]. \tag{2}$$

For SISA, the same performance guarantee is  $\mathbb{P}\left[F_r(\text{SISA}) \geq F(k)\right] = (1 - k/L)^r$ .

The proof is presented in Appendix A.3. The above result demonstrates that compared to SISA S<sup>3</sup>T significantly enhances performance by increasing the probability that the system maintains at least F(k) performance by a factor of B'. This shows that increasing the training budget B helps improve the performance of the unlearning system. Another takeaway from the above lemma is that to ensure the system performance of F(k), there is no point in increasing the budget B beyond  $\binom{L}{k}$ .

# 4 Experiments

In this section, we outline the experimental setup and evaluate the unlearning performance of  $S^3T$  across various setups. The goal of the experiments is to evaluate the functioning of individual components and the unlearning capabilities of  $S^3T$ . Specifically, we design experiments to answer the following research questions:

- (**RQ1**) Does S<sup>3</sup>T training (Section 3.2) impact the model's performance compared to full training?
- (**RQ2**) Does S<sup>3</sup>T enhance the deletion capabilities of unlearning, and what is its cost tradeoff?
- (**RQ3**) Is the sequence permutation selection algorithm (Section 3.3) effective in practice?

#### 4.1 Sequential Slice-wise Training Performance

In this section, we evaluate the effectiveness of slice-wise training. The objective of the experimental setup is to demonstrate that S<sup>3</sup>T can achieve performance comparable to full training. Note that S<sup>3</sup>T is not designed as a new fine-tuning technique that outperforms the baselines. The goal of S<sup>3</sup>T is to achieve parameter isolation for data slices without impacting the overall performance. We perform a range of experiments with different Transformer model sizes ranging from 86M up to 13B. We provide the details of the experimental setup and hyperparameters in Appendix C.1.

In Figure 5, we report the performance of fine-tuning on vision, GLUE, and SuperGLUE benchmarks. We use ViT<sub>BASE</sub> [15] (for CIFAR10 & CIFAR100 [34]), ViT<sub>LARGE</sub> (for Tiny ImageNet [38]), and RoBERTa<sub>LARGE</sub> [42] (for GLUE [62] & SuperGLUE [61]). We observe that S<sup>3</sup>T achieves comparable performance to full training (FT) across all settings. In some of the settings, we also observe that S<sup>3</sup>T is able to outperform FT (e.g., S<sup>3</sup>T obtains 2.5% accuracy gain on TinyImagenet using ViT-large). Next, we conduct experiments to evaluate the effectiveness of S<sup>3</sup>T while using large language models (LLMs). Specifically, we perform instruction tuning of Llama2-7B [60], Llama2-13B, and Llama3-8B using Alpaca dataset [55]. Then, we evaluate each instruction-tuned model on a range of tasks to evaluate the model's general/world knowledge (MMLU [29], OpenBookQA [44]), truthfulness in QA (TruthfulQA [39]), and commonsense reasoning (PIQA [6], HellaSwag [67], Winogrande [50], ARC [12]). We use LLM-evaluation suite [20] to report the performance and report the zero-shot performance for all datasets. Similar to the previous setup, in Table 1, we observe that S<sup>3</sup>T achieves comparable performance to full finetuning across all datasets and even outperforms FT on many

Table 1: Performance comparison of LLMs before and after instruction tuning using Alpaca dataset. We report the performance of Llama2-7B, Llama2-13B, and Llama3-8B models for the following settings: pre-trained model, full Training (FT), and slice-wise training (S<sup>3</sup>T). We observe S<sup>3</sup>T achieves comparable performance to FT, even outperforming FT's performance in several datasets. This shows that S<sup>3</sup>T allows parameter isolation without affecting the task performance.

Model	MMLU	HellaSwag	PIQA	Winogrande	ARC-c	ARC-e	TruthfulQA	OBQA
Llama2-7B Llama2-7B (FT) Llama2-7B (S³T)	41.3 <sub>(0.4)</sub> 43.3 <sub>(0.4)</sub> <b>43.6</b> <sub>(0.4)</sub>	76.0 <sub>(0.4)</sub> 77.4 <sub>(0.4)</sub> <b>77.7</b> <sub>(0.4)</sub>	79.1 <sub>(1.0)</sub> <b>79.9</b> <sub>(0.9)</sub> <u>79.7</u> <sub>(0.9)</sub>	69.1 <sub>(1.3)</sub> 69.6 <sub>(1.3)</sub> <b>70.5</b> <sub>(1.3)</sub>	46.3 <sub>(1.5)</sub> 50.4 <sub>(1.5)</sub> <b>51.4</b> <sub>(1.5)</sub>		39.0 <sub>(1.4)</sub> <b>46.3</b> <sub>(1.6)</sub> 43.0 <sub>(1.5)</sub>	44.2 <sub>(2.2)</sub> <b>46.8</b> <sub>(2.2)</sub> <u>46.4<sub>(2.2)</sub></u>
Llama2-13B Llama2-13B (FT) Llama2-13B (S³T)	50.5 <sub>(0.4)</sub> <b>51.8<sub>(0.4)</sub></b> <u>51.6<sub>(0.4)</sub></u>	79.4 <sub>(0.4)</sub> <b>81.3</b> <sub>(0.4)</sub> <u>80.9</u> <sub>(0.4)</sub>	80.5 <sub>(0.9)</sub> <b>82.0</b> <sub>(0.9)</sub> <u>81.8</u> <sub>(0.9)</sub>	72.2 <sub>(1.3)</sub> 72.2 <sub>(1.3)</sub> <b>72.8</b> <sub>(1.3)</sub>	49.0 <sub>(1.5)</sub> <b>55.0</b> <sub>(1.5)</sub> 54.5 <sub>(1.5)</sub>	()	36.9 <sub>(1.4)</sub> 38.8 <sub>(1.5)</sub> <b>39.6</b> <sub>(1.5)</sub>	45.2 <sub>(2.2)</sub> <b>46.6</b> <sub>(2.2)</sub> <u>46.2<sub>(2.2)</sub></u>
Llama3-8B Llama3-8B (FT) Llama3-8B (S³T)	62.2 <sub>(0.4)</sub> 59.2 <sub>(0.4)</sub> <b>59.6</b> <sub>(0.4)</sub>	79.1 <sub>(0.4)</sub> <b>80.8</b> <sub>(0.4)</sub> <u>80.2<sub>(0.4)</sub></u>	80.6 <sub>(0.9)</sub> 80.9 <sub>(0.9)</sub> <b>82.4</b> <sub>(0.9)</sub>	73.6 <sub>(1.2)</sub> 72.2 <sub>(1.3)</sub> <b>73.8</b> <sub>(1.2)</sub>	53.2 <sub>(1.5)</sub> <b>59.0</b> <sub>(1.4)</sub> 57.0 <sub>(1.5)</sub>		43.9 <sub>(1.4)</sub> 46.6 <sub>(1.6)</sub> <b>48.5</b> <sub>(1.6)</sub>	45.0 <sub>(2.2)</sub> 46.8 <sub>(2.2)</sub> <b>47.0</b> <sub>(2.2)</sub>

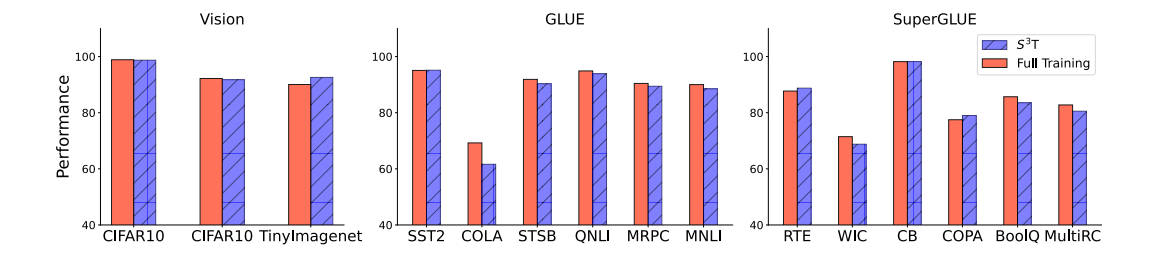


Figure 5: Comparison of the performance between slice-wise training and full training on vision datasets and GLUE & SuperGLUE benchmarks. We report the overall Matthew's correlation for CoLA, Pearson correlation for STS-B, and accuracy for other tasks. We observe that slice-wise training achieves similar performance to full training across all datasets.

datasets across different model sizes. These experiments provide the answer to (**RQ1**) demonstrating that S<sup>3</sup>T is an effective way to fine-tune Transformer models, enabling us to achieve parameter isolation for data slices without impacting the model's performance.

#### 4.2 Deletion Performance

In this section, we evaluate the performance of  $S^3T$  as deletion requests are received. In Figure 6 (left), we report the performance of  $S^3T$  and baseline SISA (with m=5 shards, L=4 slices) on CIFAR-10 and CIFAR-100 datasets. We report  $S^3T$ 's performance under various budgets. We observe that  $S^3T$  can achieve very close performance to the full budget (B=24) with a significantly smaller budget, B=4. We also observe that  $S^3T$  can handle more deletion requests and consistently outperforms the performance of the baseline method, SISA.

Next, we extensively evaluate the impact of increasing the training budget B on the deletion rate. In Figure 6 (right), we observe that there is a steady growth in the deletion rate with an increasing budget. The growth is slightly higher in the initial stages when the budget is low and slows down gradually. This experiment provides empirical evidence to our theoretical result in Lemma 3, which claims that the performance improves with an increased budget.

#### 4.3 Analysis

In this section, we conduct analysis experiments to evaluate different components within S<sup>3</sup>T.<sup>2</sup>

**Deletion Ablations**. We evaluate the deletion capabilities of  $S^3T$  and compare with the theoretical bounds. In Figure 7 (left), we report the deletion rate of  $S^3T$  and SISA for the setup (with m=5

<sup>&</sup>lt;sup>2</sup>Apart from these experiments, we also report several other analysis experiments in Appendix C.2.

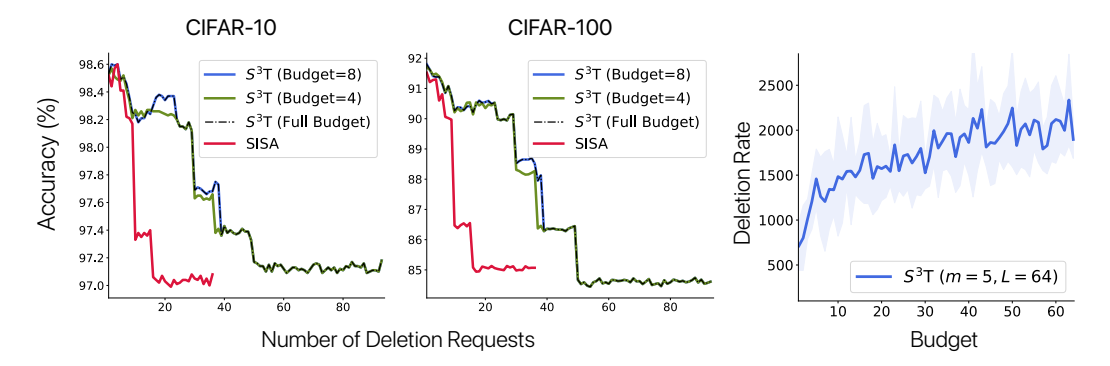


Figure 6: (*Left*) We report the impact on performance of  $S^3T$  and baselines with an increasing number of deletion requests. We observe that  $S^3T$  can handle a higher number of deletion requests while maintaining high performance with a relatively low budget. (*Right*) We report the deletion rate of  $S^3T$  with an increasing budget and observe steady growth.

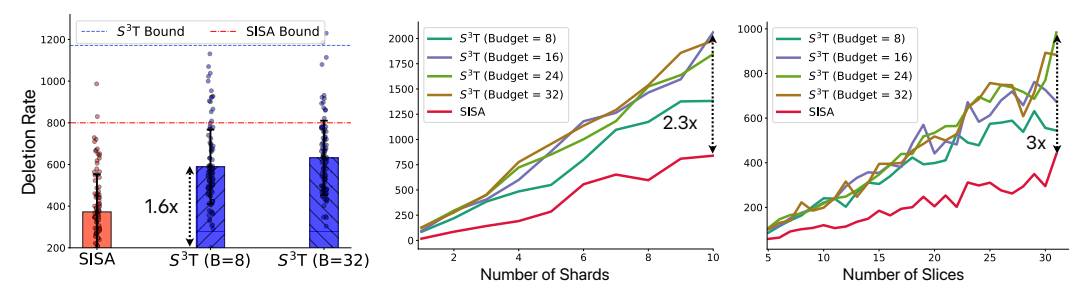


Figure 7: We report the deletion rate of S<sup>3</sup>T and compare it with the baselines. (*Left*) We compare the deletion rates of S<sup>3</sup>T under varying budgets with SISA and observe significant gains. (*Center*) We report the deletion rates with increasing number of shards and (*Right*) an increasing number of slices. In both scenarios, we observe that the deletion rate of S<sup>3</sup>T grows significantly faster than the baseline.

shards, L=32 slices). We observe that with a small budget B=8,  $S^3T$  can achieve 1.6x gains in the number of deletion requests handled. We also plot the theoretical bounds derived in Section 3.4 and show that they hold in practice. Note that increasing the budget B>L does not help improve the deletion rate but increases the probability of a better-performing model (as observed in Lemma 3).

In Figure 7 (center & right), we report the model performance with varying shard and slice counts. As expected, we observe that both increasing the shards and slicing the data more helps in improving the deletion performance. However, the rate of growth in deletion rate is more significant for S<sup>3</sup>T resulting in up to 2.3x and 3x gains over SISA for the same number of shards and slices respectively.

This shows that by using additional offline training (increased budget) it is possible to improve the deletion rate thereby reducing retraining costs.

**Sequence Selection.** We evaluate the quality of the sequences generated by the BMS algorithm (Section 3.3) and compare it with random sampling. Ideally, we want the selected sequences to be diverse and thereby compute the edit distance between sequences. Specifically,

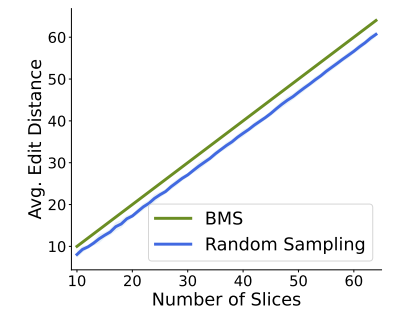


Figure 8: We evaluate the performance of bipartite matching-based selection (BMS) and observe that BMS consistently outperforms random sampling.

we report the following score for a selected subset,  $O: Q(O) = \mathbb{E}_{o \in O}[\min_{o' \in O \setminus o} d_{\text{edit}}(o, o')]$ , which measures the average minimum edit distance within the subset. In Figure 8 (left), we report the Q(O) for a varying number of slices, L. We observe that BMS consistently outperforms random sampling, which indicates that the generated sequences are more diverse.

## 5 Conclusion

In this paper, we introduced S<sup>3</sup>T, an effective framework for performing exact unlearning. S<sup>3</sup>T uses a modular machine learning model that is trained using disjoint shards of the data. Each shard is used to train a different model using a lightweight fine-tuning approach that enables parameter isolation, which allows us to execute unlearning requests efficiently. The key idea behind S<sup>3</sup>T is to train multiple models using different sequences of slices before deploying the system. This helps reduce retraining costs and improve the model's performance while the model is in production. Both theoretically and empirically, we show that S<sup>3</sup>T has significantly improved deletion capabilities compared to existing approaches. Future work can focus on developing techniques for finer-grained parameter isolation to further improve the overall performance of S<sup>3</sup>T.

# 6 Acknowledgments

The authors thank Vinayshekhar Bannihatti Kumar, Nicholas Monath, and Shounak Chattopadhyay for helpful feedback and discussions.

#### 7 Author Contributions

SBRC proposed the unlearning idea, conducted all the experiments and led the project. KC proposed the diverse permutation selection algorithm using bipartite graph matching. AS contributed to deriving the theoretical results and designing the empirical studies. AD and SC provided ideas and served as project advisors, offering extensive assistance in organizing the manuscript. All authors contributed to the writing of the manuscript.

#### References

- [1] Josh Achiam, Steven Adler, Sandhini Agarwal, Lama Ahmad, Ilge Akkaya, Florencia Leoni Aleman, Diogo Almeida, Janko Altenschmidt, Sam Altman, Shyamal Anadkat, et al. Gpt-4 technical report. *arXiv preprint arXiv:2303.08774*, 2023.
- [2] Alessandro Achille, Michael Kearns, Carson Klingenberg, and Stefano Soatto. Ai model disgorgement: Methods and choices. *Proceedings of the National Academy of Sciences*, 121(18):e2307304121, 2024.
- [3] Nasser Aldaghri, Hessam Mahdavifar, and Ahmad Beirami. Coded machine unlearning. *IEEE Access*, 9:88137–88150, 2021.
- [4] P Bhattacharya. The representation of permutations by trees. *Computers & Mathematics with Applications*, 28(9):67–71, 1994.
- [5] Battista Biggio, Blaine Nelson, and Pavel Laskov. Poisoning attacks against support vector machines. *arXiv preprint arXiv:1206.6389*, 2012.
- [6] Yonatan Bisk, Rowan Zellers, Jianfeng Gao, Yejin Choi, et al. Piqa: Reasoning about physical commonsense in natural language. In *Proceedings of the AAAI conference on artificial intelligence*, volume 34, pages 7432–7439, 2020.
- [7] Gunnar Blom, Lars Holst, and Dennis Sandell. 7.5 coupon collecting i, 7.6 coupon collecting ii, and 15.4 coupon collecting iii. *Problems and Snapshots from the World of Probability, New York: Springer-Verlag*, pages 85–87, 1994.
- [8] Lucas Bourtoule, Varun Chandrasekaran, Christopher A Choquette-Choo, Hengrui Jia, Adelin Travers, Baiwu Zhang, David Lie, and Nicolas Papernot. Machine unlearning. In 2021 IEEE Symposium on Security and Privacy (SP), pages 141–159. IEEE, 2021.
- [9] Tom Brown, Benjamin Mann, Nick Ryder, Melanie Subbiah, Jared D Kaplan, Prafulla Dhariwal, Arvind Neelakantan, Pranav Shyam, Girish Sastry, Amanda Askell, et al. Language models are few-shot learners. Advances in neural information processing systems, 33:1877–1901, 2020.
- [10] Yinzhi Cao and Junfeng Yang. Towards making systems forget with machine unlearning. In 2015 IEEE symposium on security and privacy, pages 463–480. IEEE, 2015.

- [11] Jiaao Chen and Diyi Yang. Unlearn what you want to forget: Efficient unlearning for Ilms. In *The 2023 Conference on Empirical Methods in Natural Language Processing*, 2023.
- [12] Peter Clark, Isaac Cowhey, Oren Etzioni, Tushar Khot, Ashish Sabharwal, Carissa Schoenick, and Oyvind Tafjord. Think you have solved question answering? try arc, the ai2 reasoning challenge. *arXiv preprint arXiv:1803.05457*, 2018.
- [13] Thomas H Cormen, Charles E Leiserson, Ronald L Rivest, and Clifford Stein. *Introduction to algorithms*. MIT press, 2022.
- [14] Jacob Devlin, Ming-Wei Chang, Kenton Lee, and Kristina Toutanova. BERT: Pre-training of deep bidirectional transformers for language understanding. In Jill Burstein, Christy Doran, and Thamar Solorio, editors, Proceedings of the 2019 Conference of the North American Chapter of the Association for Computational Linguistics: Human Language Technologies, Volume 1 (Long and Short Papers), pages 4171–4186, Minneapolis, Minnesota, June 2019. Association for Computational Linguistics.
- [15] Alexey Dosovitskiy, Lucas Beyer, Alexander Kolesnikov, Dirk Weissenborn, Xiaohua Zhai, Thomas Unterthiner, Mostafa Dehghani, Matthias Minderer, Georg Heigold, Sylvain Gelly, et al. An image is worth 16x16 words: Transformers for image recognition at scale. In *International Conference on Learning Representations*, 2020.
- [16] Yonatan Dukler, Benjamin Bowman, Alessandro Achille, Aditya Golatkar, Ashwin Swaminathan, and Stefano Soatto. Safe: Machine unlearning with shard graphs. In *Proceedings of the IEEE/CVF International Conference on Computer Vision*, pages 17108–17118, 2023.
- [17] Ronen Eldan and Mark Russinovich. Who's harry potter? approximate unlearning in llms. *arXiv preprint arXiv:2310.02238*, 2023.
- [18] European Parliament and Council of the European Union. Regulation (EU) 2016/679 of the European Parliament and of the Council.
- [19] Zvi Galil. Efficient algorithms for finding maximum matching in graphs. *ACM Computing Surveys (CSUR)*, 18(1):23–38, 1986.
- [20] Leo Gao, Jonathan Tow, Baber Abbasi, Stella Biderman, Sid Black, Anthony DiPofi, Charles Foster, Laurence Golding, Jeffrey Hsu, Alain Le Noac'h, Haonan Li, Kyle McDonell, Niklas Muennighoff, Chris Ociepa, Jason Phang, Laria Reynolds, Hailey Schoelkopf, Aviya Skowron, Lintang Sutawika, Eric Tang, Anish Thite, Ben Wang, Kevin Wang, and Andy Zou. A framework for few-shot language model evaluation, 12 2023.
- [21] Alan Gibbons. Algorithmic graph theory. Cambridge university press, 1985.
- [22] Aditya Golatkar, Alessandro Achille, and Stefano Soatto. Eternal sunshine of the spotless net: Selective forgetting in deep networks. In *Proceedings of the IEEE/CVF Conference on Computer Vision and Pattern Recognition*, pages 9304–9312, 2020.
- [23] Aditya Golatkar, Alessandro Achille, and Stefano Soatto. Forgetting outside the box: Scrubbing deep networks of information accessible from input-output observations. In *European Conference on Computer Vision*, pages 383–398, 2020.
- [24] Aditya Golatkar, Alessandro Achille, Ashwin Swaminathan, and Stefano Soatto. Training data protection with compositional diffusion models. *arXiv preprint arXiv:2308.01937*, 2023.
- [25] Laura Graves, Vineel Nagisetty, and Vijay Ganesh. Amnesiac machine learning. In *Proceedings of the AAAI Conference on Artificial Intelligence*, volume 35, pages 11516–11524, 2021.
- [26] Chuan Guo, Tom Goldstein, Awni Hannun, and Laurens Van Der Maaten. Certified data removal from machine learning models. In *International Conference on Machine Learning*, pages 3832–3842. PMLR, 2020.
- [27] Varun Gupta, Christopher Jung, Seth Neel, Aaron Roth, Saeed Sharifi-Malvajerdi, and Chris Waites. Adaptive machine unlearning. *Advances in Neural Information Processing Systems*, 34:16319–16330, 2021.
- [28] Jamie Hayes, Ilia Shumailov, Eleni Triantafillou, Amr Khalifa, and Nicolas Papernot. Inexact unlearning needs more careful evaluations to avoid a false sense of privacy. *arXiv* preprint *arXiv*:2403.01218, 2024.
- [29] Dan Hendrycks, Collin Burns, Steven Basart, Andy Zou, Mantas Mazeika, Dawn Song, and Jacob Steinhardt. Measuring massive multitask language understanding. In *International Conference on Learning Representations*, 2020.

- [30] John E Hopcroft and Richard M Karp. An n<sup>5</sup>/2 algorithm for maximum matchings in bipartite graphs. *SIAM Journal on computing*, 2(4):225–231, 1973.
- [31] Edward J Hu, Phillip Wallis, Zeyuan Allen-Zhu, Yuanzhi Li, Shean Wang, Lu Wang, Weizhu Chen, et al. Lora: Low-rank adaptation of large language models. In *International Conference on Learning Representations*, 2021.
- [32] Jinghan Jia, Jiancheng Liu, Parikshit Ram, Yuguang Yao, Gaowen Liu, Yang Liu, Pranay Sharma, and Sijia Liu. Model sparsification can simplify machine unlearning. *arXiv* preprint *arXiv*:2304.04934, 2023.
- [33] Pang Wei Koh and Percy Liang. Understanding black-box predictions via influence functions. In *International conference on machine learning*, pages 1885–1894. PMLR, 2017.
- [34] Alex Krizhevsky, Geoffrey Hinton, et al. Learning multiple layers of features from tiny images. 2009.
- [35] Vinayshekhar Bannihatti Kumar, Rashmi Gangadharaiah, and Dan Roth. Privacy adhering machine un-learning in nlp. In *Findings of the Association for Computational Linguistics: IJCNLP-AACL 2023 (Findings)*, pages 268–277, 2023.
- [36] Meghdad Kurmanji, Peter Triantafillou, Jamie Hayes, and Eleni Triantafillou. Towards unbounded machine unlearning. *Advances in Neural Information Processing Systems*, 36, 2024.
- [37] Jeffrey Lagarias. Euler's constant: Euler's work and modern developments. *Bulletin of the American Mathematical Society*, 50(4):527–628, 2013.
- [38] Ya Le and Xuan Yang. Tiny imagenet visual recognition challenge. CS 231N, 7(7):3, 2015.
- [39] Stephanie Lin, Jacob Hilton, and Owain Evans. TruthfulQA: Measuring how models mimic human falsehoods. In Smaranda Muresan, Preslav Nakov, and Aline Villavicencio, editors, *Proceedings of the 60th Annual Meeting of the Association for Computational Linguistics* (*Volume 1: Long Papers*), pages 3214–3252, Dublin, Ireland, May 2022. Association for Computational Linguistics.
- [40] Jiaqi Liu, Jian Lou, Zhan Qin, and Kui Ren. Certified minimax unlearning with generalization rates and deletion capacity. Advances in Neural Information Processing Systems, 36, 2024.
- [41] Sijia Liu, Yuanshun Yao, Jinghan Jia, Stephen Casper, Nathalie Baracaldo, Peter Hase, Xiaojun Xu, Yuguang Yao, Hang Li, Kush R Varshney, et al. Rethinking machine unlearning for large language models. *arXiv preprint arXiv:2402.08787*, 2024.
- [42] Yinhan Liu, Myle Ott, Naman Goyal, Jingfei Du, Mandar Joshi, Danqi Chen, Omer Levy, Mike Lewis, Luke Zettlemoyer, and Veselin Stoyanov. Roberta: A robustly optimized bert pretraining approach. *arXiv preprint arXiv:1907.11692*, 2019.
- [43] Alessandro Mantelero. The eu proposal for a general data protection regulation and the roots of the 'right to be forgotten'. *Computer Law & Security Review*, 29(3):229–235, 2013.
- [44] Todor Mihaylov, Peter Clark, Tushar Khot, and Ashish Sabharwal. Can a suit of armor conduct electricity? a new dataset for open book question answering. In *Conference on Empirical Methods in Natural Language Processing*, 2018.
- [45] Seth Neel, Aaron Roth, and Saeed Sharifi-Malvajerdi. Descent-to-delete: Gradient-based methods for machine unlearning. In *Algorithmic Learning Theory*, pages 931–962. PMLR, 2021.
- [46] Thanh Tam Nguyen, Thanh Trung Huynh, Phi Le Nguyen, Alan Wee-Chung Liew, Hongzhi Yin, and Quoc Viet Hung Nguyen. A survey of machine unlearning. arXiv preprint arXiv:2209.02299, 2022.
- [47] Adam Paszke, Sam Gross, Francisco Massa, Adam Lerer, James Bradbury, Gregory Chanan, Trevor Killeen, Zeming Lin, Natalia Gimelshein, Luca Antiga, et al. Pytorch: An imperative style, high-performance deep learning library. *Advances in neural information processing systems*, 32, 2019.
- [48] Vaidehi Patil, Peter Hase, and Mohit Bansal. Can sensitive information be deleted from llms? objectives for defending against extraction attacks. In *The Twelfth International Conference on Learning Representations*, 2023.

- [49] Adnan Qayyum, Junaid Qadir, Muhammad Bilal, and Ala Al-Fuqaha. Secure and robust machine learning for healthcare: A survey. IEEE Reviews in Biomedical Engineering, 14:156– 180, 2020.
- [50] Keisuke Sakaguchi, Ronan Le Bras, Chandra Bhagavatula, and Yejin Choi. Winogrande: An adversarial winograd schema challenge at scale. *Communications of the ACM*, 64(9):99–106, 2021.
- [51] Ayush Sekhari, Jayadev Acharya, Gautam Kamath, and Ananda Theertha Suresh. Remember what you want to forget: Algorithms for machine unlearning. *Advances in Neural Information Processing Systems*, 34:18075–18086, 2021.
- [52] Supreeth Shastri, Melissa Wasserman, and Vijay Chidambaram. The seven sins of {Personal-Data} processing systems under {GDPR}. In 11th USENIX Workshop on Hot Topics in Cloud Computing (HotCloud 19), 2019.
- [53] Jacob Steinhardt, Pang Wei W Koh, and Percy S Liang. Certified defenses for data poisoning attacks. *Advances in neural information processing systems*, 30, 2017.
- [54] Vinith Suriyakumar and Ashia C Wilson. Algorithms that approximate data removal: New results and limitations. Advances in Neural Information Processing Systems, 35:18892–18903, 2022.
- [55] Rohan Taori, Ishaan Gulrajani, Tianyi Zhang, Yann Dubois, Xuechen Li, Carlos Guestrin, Percy Liang, and Tatsunori B. Hashimoto. Stanford alpaca: An instruction-following llama model. https://github.com/tatsu-lab/stanford\_alpaca, 2023.
- [56] Ayush K Tarun, Vikram S Chundawat, Murari Mandal, and Mohan Kankanhalli. Fast yet effective machine unlearning. *IEEE Transactions on Neural Networks and Learning Systems*, 2023.
- [57] Ayush Kumar Tarun, Vikram Singh Chundawat, Murari Mandal, and Mohan Kankanhalli. Deep regression unlearning. In *International Conference on Machine Learning*, pages 33921–33939. PMLR, 2023.
- [58] Gemini Team, Rohan Anil, Sebastian Borgeaud, Yonghui Wu, Jean-Baptiste Alayrac, Jiahui Yu, Radu Soricut, Johan Schalkwyk, Andrew M Dai, Anja Hauth, et al. Gemini: a family of highly capable multimodal models. *arXiv preprint arXiv:2312.11805*, 2023.
- [59] Anvith Thudi, Hengrui Jia, Ilia Shumailov, and Nicolas Papernot. On the necessity of auditable algorithmic definitions for machine unlearning. In 31st USENIX Security Symposium (USENIX Security 22), pages 4007–4022, 2022.
- [60] Hugo Touvron, Louis Martin, Kevin Stone, Peter Albert, Amjad Almahairi, Yasmine Babaei, Nikolay Bashlykov, Soumya Batra, Prajjwal Bhargava, Shruti Bhosale, et al. Llama 2: Open foundation and fine-tuned chat models. *arXiv preprint arXiv:2307.09288*, 2023.
- [61] Alex Wang, Yada Pruksachatkun, Nikita Nangia, Amanpreet Singh, Julian Michael, Felix Hill, Omer Levy, and Samuel Bowman. Superglue: A stickier benchmark for general-purpose language understanding systems. *Advances in neural information processing systems*, 32, 2019.
- [62] Alex Wang, Amanpreet Singh, Julian Michael, Felix Hill, Omer Levy, and Samuel Bowman. Glue: A multi-task benchmark and analysis platform for natural language understanding. In *Proceedings of the 2018 EMNLP Workshop BlackboxNLP: Analyzing and Interpreting Neural Networks for NLP*, pages 353–355, 2018.
- [63] Cheng-Long Wang, Qi Li, Zihang Xiang, and Di Wang. Has approximate machine unlearning been evaluated properly? from auditing to side effects. *arXiv preprint arXiv:2403.12830*, 2024.
- [64] Thomas Wolf, Lysandre Debut, Victor Sanh, Julien Chaumond, Clement Delangue, Anthony Moi, Pierric Cistac, Tim Rault, Rémi Louf, Morgan Funtowicz, et al. Huggingface's transformers: State-of-the-art natural language processing. arXiv preprint arXiv:1910.03771, 2019.
- [65] Heng Xu, Tianqing Zhu, Lefeng Zhang, Wanlei Zhou, and Philip S. Yu. Machine unlearning: A survey. *ACM Comput. Surv.*, 56(1), aug 2023.
- [66] Haonan Yan, Xiaoguang Li, Ziyao Guo, Hui Li, Fenghua Li, and Xiaodong Lin. Arcane: An efficient architecture for exact machine unlearning. In *IJCAI*, volume 6, page 19, 2022.
- [67] Rowan Zellers, Ari Holtzman, Yonatan Bisk, Ali Farhadi, and Yejin Choi. Hellaswag: Can a machine really finish your sentence? In *Proceedings of the 57th Annual Meeting of the Association for Computational Linguistics*, pages 4791–4800, 2019.

#### A Mathematical Proofs

#### **Contents**

<b>A.</b> 1	Proof of Lemma 1	14
A.2	Proof of Lemma 2	14
A.3	Proof of Lemma 3	15

## A.1 Proof of Lemma 1

This lemma states that BMS is optimal and selects diverse sequences. Two sequences are considered diverse if no element appears at the same position, e.g.,  $(S_1, S_2, S_3, S_4)$  and  $(S_2, S_3, S_4, S_1)$ . Since we want diverse sequences, BMS performs perfect matching, ensuring that no two elements appear in the same position. Therefore, in this proof, we show that perfect matching exists at all levels, [1, L], in Algorithm 1.

*Proof.* Let the bipartite graph, G, consist of vertices  $V \cup V'$ , such that the edges  $E \subseteq V \times V'$ . For a perfect matching to exist, every subset  $W \subset V$  should satisfy:

$$|W| \le N_G(W),\tag{3}$$

where  $N_G(\cdot)$  is the neighbourhood defined using the graph, G.

In our setup, the graph G has vertices  $V=\{1,\ldots,L\}$  and  $V'=\{1',\ldots,L'\}$ , which indicate the elements in the permutation sequence. Every vertex  $v\in V$  has (L-i+1) edges to unique vertices in V' at the i-th iteration of the algorithm. Therefore, for all iterations  $i\in\{2,\ldots,L\}$  (shown in Line 6 in Algorithm 1) the condition in Eq. 3 is satisfied and a perfect matching exists.

Since perfect matching selects a unique element in V', therefore no element is repeated at the same position in the BMS output. This happens for all iterations, BMS is optimal.

#### A.2 Proof of Lemma 2

In S<sup>3</sup>T, when  $B \ge L$  then all slices  $\{1, \dots, L\}$  must occupy the topmost position in one of the trained models (an example is shown in Figure 4). This implies that for S<sup>3</sup>T to encounter service failure, all slices in all shards must be affected by deletion requests. Therefore, considering deletion requests affect all slices uniformly we need to compute the expected time till all slices are affected. This setup is similar to the coupon collector problem [7].

*Proof.* The deletion rate is the expected number of requests to delete all mL slices (m shards, L slices per shard). Using linearity of expectation, the deletion rate or total time can be written as:

$$\delta(S^{3}T) = \mathbb{E}[T] = \mathbb{E}[t_{1} + \ldots + t_{mL}] \tag{4}$$

$$= \mathbb{E}[t_1] + \ldots + \mathbb{E}[t_{mL}], \tag{5}$$

where  $\mathbb{E}[t_i] = 1/p_i$ , where  $p_i$  is the probability that the *i*-th slice is affected after (i-1) slices are deleted. Let  $N = |\mathcal{D}|$  the dataset size and r be the number of deletion requests seen so far. The expression of  $p_i$  is shown below:

$$p_i = \frac{\{mL - (i-1)\}s_b}{N - r} = \frac{N - (i-1)s_b}{N - r} = \frac{1 - (i-1)/mL}{1 - r/N} \ge \frac{mL - (i-1)}{mL},\tag{6}$$

where  $s_b$  is the size of each slice. Replacing this result in Eq. 5, we get:

$$\delta(\mathbf{S}^{3}\mathbf{T}) \le \frac{mL}{mL - 0} + \frac{mL}{mL - 1} + \ldots + \frac{mL}{1}$$

$$\tag{7}$$

$$= mL\left(\frac{1}{1} + \frac{1}{2} + \ldots + \frac{1}{mL}\right) \tag{8}$$

$$= mL.H_{mL} \tag{9}$$

$$= mL\log(mL) + \gamma mL + \frac{1}{2} + O\left(\frac{1}{mL}\right),\tag{10}$$

where  $H_{mL}$  denotes the mL-th Harmonic number and  $\gamma$  is the Euler's constant [37]. The above result proves the first portion of the lemma,  $\delta(S^3T) \sim O(mL \log mL)$ .

The second part of the lemma is about SISA. For SISA to experience failure, only the first slice of each shard (total of m slices) needs to be affected by deletion. In this case, we can write:

$$p_i = \frac{\{m - (i-1)\}s_b}{N - r} = \frac{N/L - (i-1)s_b}{N - r} = \frac{1 - (i-1)/m}{L(1 - r/N)} \ge \frac{m - (i-1)}{mL}$$
(11)

Replacing the above result in Eq. 5, we get:

$$\delta(SISA) \le mL\left(\frac{1}{1} + \frac{1}{2} + \dots + \frac{1}{m}\right) \tag{12}$$

$$= mL.H_m \tag{13}$$

$$= mL\log(m) + \gamma m + \frac{1}{2} + O\left(\frac{1}{m}\right). \tag{14}$$

This proves the second portion of the lemma:  $\delta(SISA) \sim O(mL \log m)$ .

## A.3 Proof of Lemma 3

We begin by proving the retention result for SISA as it is simpler to understand. Each model within SISA is trained on a single sequence of slices.

*Proof.* The probability it maintains performs better than F(k) is equivalent to showing that none of the top-k elements (out of L) are affected after r deletion requests:

$$\mathbb{P}\left[F_r(\text{SISA}) \ge F(k)\right] = \left(1 - \frac{k}{L}\right)^r. \tag{15}$$

In  $S^3T$ , each model is trained on B such sequences. Therefore, the probability that all B sequences are affected is:

$$\mathbb{P}\left[F_r(\mathbf{S}^3\mathbf{T}) \ge F(k)\right] = B\left(1 - \frac{k}{L}\right)^r. \tag{16}$$

However, the above result suggests that the probability can be increased indefinitely by increasing B, which is not accurate because there are only  $\binom{L}{k}$  possible sequences. To correct this, we show:

$$\mathbb{P}\left[F_r(\mathbf{S}^3\mathbf{T}) \ge F(k)\right] = B'\left(1 - \frac{k}{L}\right)^r,\tag{17}$$

where  $B' = \min \left\{ B, \binom{L}{k} \right\}$ . This proves the lemma.

# **B** Implementation Details

In this section, we discuss the details of various algorithms and workflows within S<sup>3</sup>T.

#### **Contents**

B.1	Bipartite-matching based Sequence Selection										16
B.2	S <sup>3</sup> T Training Procedure										16
B.3	Deletion Procedure										17

#### **B.1** Bipartite-matching based Sequence Selection

We describe the details of the Bipartite-matching based selection (BMS) algorithm in Algorithm 1. The objective of BMS is to select a set of B diverse permutation sequences of length L (slice count). This algorithm starts by selecting L different starting elements for the sequences in Line 4. Then, BMS iteratively selects the next element within each sequence. This involves constructing a bipartite graph between the last elements of the sequences seen so far and the next set of elements. The edges incident on feasible next elements (elements not seen in a permutation sequence so far) as shown in Line 11. We perform bipartite graph matching on the graph, G. Based on the matching, we select the next element for each permutation sequence (Line 17). BMS continues this process till all sequences  $o \in \mathcal{O}$  have L elements. Based on the budget, we output B sequences from  $\mathcal{O}$ .

For Bipartite graph matching, Hopcroft–Karp algorithm [30] provides an efficient algorithm with time complexity  $O(|E|\sqrt{|V|})$ , where |E|,|V| are the number of edges and vertices respectively. Using this algorithm, the overall time complexity of BMS is  $O(L^{2.5})$ .

## **Algorithm 1** BMS Sequence Selection Algorithm

```
1: function BMS(Slice count: L, Budget: B)
 2:
         for l \in \{1,\dots,L\} do // initializing the sequence set with first element
 3:
              \mathcal{O} = \mathcal{O} \cup \{l\}
 4:
 5:
         end for
         for i \in \{2, ..., L\} do // iterations to select the 2^{\text{nd}} to the L-th element
 6:
 7:
              G = \{\} // Initialize Graph
              for o \in \mathcal{O} do // Iterate over sequences
 8:
 9:
                  v = o.pop() // Collect final element of each sequence
                  for v' \in \{1, \dots, L\} do // Iterate and add all feasible edges
10:
                       if v' \notin o then G.add_edge(v, v') // check for feasibility
11:
                  end for
12:
              end for
13:
14:
              (V, V') = \operatorname{PerfectMatching}(G) // \operatorname{compute bipartite perfect matching}[30]
15:
16:
                  // select vertex associated with each sequence from perfect matching
                  v^* = \{v' | v' \in V' \land v = o.pop()\}
17:
18:
                  o = o \cup v^* // add to sequence
19:
              end for
20:
         end for
         \mathcal{O}_B = \{o_1, \dots, o_B\} \in \mathcal{O} // \text{ select any } B \text{ sequences from } \mathcal{O}
21:
22:
         return \mathcal{O}_B
23: end function
```

#### **B.2** S<sup>3</sup>T Training Procedure

In this section, we provide an outline for the training procedure within the S<sup>3</sup>T framework in Algorithm 2. S<sup>3</sup>T proceeds by dividing the entire dataset into m shards. Each shard is further divided into L disjoint slices. Based on the budget B, we obtain the permutation sequences to perform slice-wise training. We train each model f on a unique sequence of slice sequence,  $\pi(S)$ . We return

#### **Algorithm 2** S<sup>3</sup>T Training Procedure

```
1: Input: Dataset \mathcal{D}, Shard Count: m, Slice Count: L, Budget: B
 2: \mathcal{F} = \{\} // initializing model set
 3: for d \in \{\mathcal{D}_1, \dots, \mathcal{D}_m\} do // partition the dataset into shards and iterate over them
         S = \{S_1, \dots, S_L\} // partition into slices, \cup_i S = d
 5:
         if B \le L then
              \Pi = BMS(L, B) // perform BMS selection
 6:
 7:
 8:
              \Pi = \text{ConditionalSampling}(L, B) // \text{Conditional Sampling based selection}
 9:
         end if
10:
         for \pi \in \Pi do
             S_{\pi} = \pi(S) // order the slices according to the permutation \pi
11:
              f = \hat{\text{SliceWiseTraining}}(S_{\pi})
12:
              \mathcal{F} = \mathcal{F} \cup f
13:
         end for
14:
15: end for
16: return \mathcal{F}
```

# **Algorithm 3** S<sup>3</sup>T Deletion Procedure

```
1: Input: Model set \mathcal{F}, Deletion instance: x
 2: m' = \text{LocateShard}(x) // \text{ get original shard ID}, m'
 3: \overline{\mathcal{F}} = \{\} // set of modified models
 4: for f \in \mathcal{F}_{m'} do // iterate over models trained on m'-th shard
 5:
          l' = \text{LocateSlice}(x, f) // get original slice ID, l', of x within f
          for l \in \{l', \ldots, L\} do
 6:
                DeactivateLayer(f, l) // deactivate PEFT layers
 7:
 8:
          if l' > 0 then \overline{\mathcal{F}} = \overline{\mathcal{F}} \cup f // ensuring all layers aren't switched off
 9:
10: end for
11: \mathcal{F} = \mathcal{F} \setminus \mathcal{F}_{m'} // remove older models
12: \mathcal{F} = \mathcal{F} \setminus \overline{\mathcal{F}} // introduce updated models
13: return \mathcal{F}
```

the complete set of models,  $\mathcal{F}$ . During inference, the user selects the best performing model within each shard and deploys an ensemble of those models to production.

## **B.3** Deletion Procedure

In this section, we describe the procedure when a deletion request arrives for an instance x in Algorithm 3. We first locate the shard ID, m', where the instance x belonged and iterate over all models trained on that shard. For each of these models, we locate the slice ID, l', of x and deactivate all layers  $\{l', \ldots, L\}$  (as shown in Line 7). After that, if the model f is still active, we add it to the set of modified models,  $\overline{\mathcal{F}}$ . S<sup>3</sup>T uses the updated set to perform inference till a new deletion request arrives. Note that the deletion process can occur entirely offline without impacting the production system, provided that the deleted instance does not influence any of the ensemble models.

Table 2: We report the hyperparameters used in our experiments for fine-tuning S<sup>3</sup>T across different benchmarks and Transformer model variants.

		# SLICES	# LAYERS/	Lora	LoRA	LEARNING			
DATASET	MODEL	(L)	SLICE	RANK $(r)$		RATE	EPOCHS		
GLUE Benchmark									
SST-2	RoBERTa <sub>LARGE</sub>	7	3	16	32	$10^{-5}$	10		
COLA	RoBERTa <sub>LARGE</sub>	7	2	8	16	$4.10^{-4}$	30		
STS-B	RoBERTa <sub>LARGE</sub>	7	3	16	32	$10^{-4}$	30		
QNLI	RoBERTa <sub>LARGE</sub>	7	3	8	16	$5.10^{-5}$	30		
QQP	RoBERTa <sub>LARGE</sub>	7	3	16	32	$5.10^{-5}$	30		
MRPC	RoBERTa <sub>LARGE</sub>	7	3	16	32	$5.10^{-5}$	30		
MNLI	$RoBERTa_{LARGE}$	7	3	16	32	$10^{-4}$	30		
SuperGLUE Benchmar	k								
RTE	RoBERTa <sub>LARGE</sub>	8	4	16	32	$10^{-5}$	30		
WIC	RoBERTa <sub>LARGE</sub>	12	2	16	32	$10^{-4}$	30		
CB	RoBERTa <sub>LARGE</sub>	12	2	16	32	$10^{-4}$	30		
COPA	RoBERTa <sub>LARGE</sub>	12	2	32	64	$10^{-5}$	30		
BoolQ	RoBERTa <sub>LARGE</sub>	7	3	16	32	$10^{-4}$	30		
MultiRC	$RoBERTa_{LARGE}$	7	3	16	32	$10^{-4}$	30		
Vision Benchmark									
CIFAR-10	ViT <sub>BASE</sub>	6	2	16	32	$2.10^{-3}$	15		
CIFAR-100	$ViT_{BASE}$	6	2	16	32	$2.10^{-3}$	15		
TinyImagenet	$ViT_{LARGE}$	6	4	16	32	$2.10^{-3}$	15		
<b>Instruction Tuning</b>									
Alpaca	Llama2-7B	4	8	32	64	$2.10^{-5}$	3		
Alpaca	Llama2-13B	4	10	32	64	$2.10^{-5}$	3		
Alpaca	Llama3-8B	4	8	32	64	$2.10^{-5}$	3		

# **C** Experiments

In this section, we describe our experimental setup and present additional analysis experiments to evaluate the functioning of S<sup>3</sup>T.

## C.1 Experimental Setup

We perform all experiments using PyTorch [47] and Huggingface [64] framework. Our experiments were run on NVIDIA A6000 GPUs. In Table 2, we report the common set of hyperparameters for S³T fine-tuning experiments. All hyperparameters were set using a grid search with the Weights & Biases framework. We use an AdamW optimizer with the corresponding learning rates for each dataset (reported in Table 2). During fine-tuning of the models, we perform full-precision training for all settings except instruction tuning where we use 8-bit training.

## **C.2** Additional Experiments

In this section, we report analysis experiments to evaluate the S<sup>3</sup>T's deletion capabilities and training.

**Performance Degradation with Slice Deletion**. In Figure 9, we report the relative performance drop with an increasing number of slices affected by deletion requests. For vision datasets in Figure 9 (left), we only observe a small drop in performance (<5%). For instruction tuning in Figure 9 (middle), we observe a negligible performance drop for most datasets except MMLU & ARC, which are more challenging open-ended QA benchmarks. For text classification in Figure 9 (right), we observe an increased drop in performance for a few of the datasets. We hypothesize that this occurs because the RoBERTa<sub>LARGE</sub> (used in text classification tasks) is a relatively weaker pre-trained model compared to Llama and ViT, which may explain this behavior. We also observe that the performance can vary based on the task and overall it is dependent on both the task and the model being fine-tuned. For unlearning, a lower performance drop is better as it suggests that we can continue using the same model without retraining for a longer time.

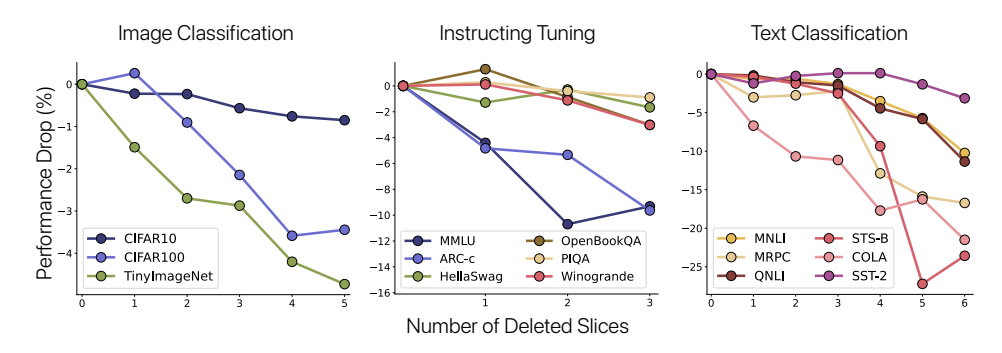


Figure 9: Relative performance drop with an increasing number of deleted slices. We observe a relatively small performance drop for image classification and instruction tuning tasks, while noticing a considerable drop for few of the text classification datasets.

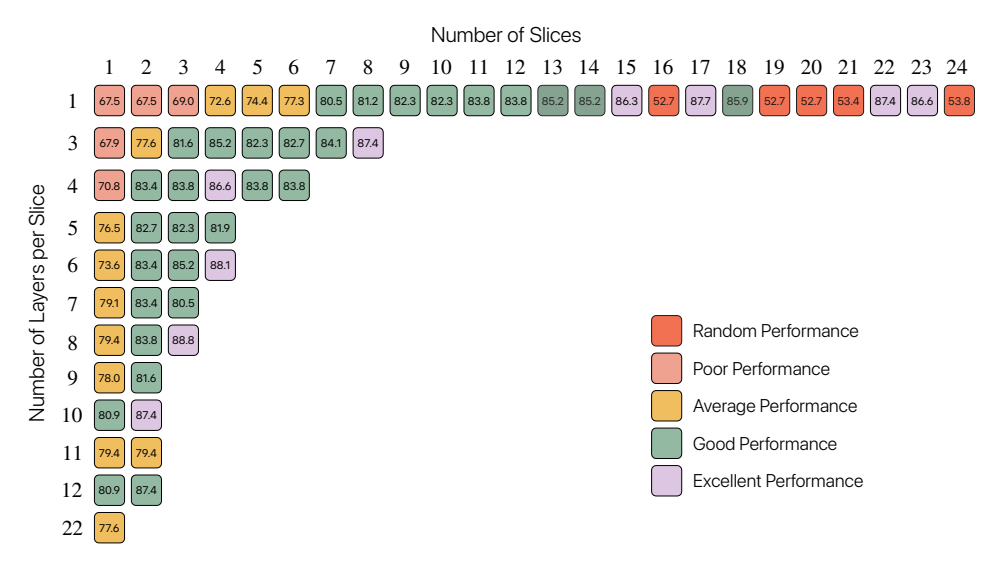


Figure 10: Performance impact of S<sup>3</sup>T when allocated a different number of layers per slice: We observe that simply increasing the number of slices can lead to a significant performance drop. There is an optimal tradeoff between the total number of slices and the number of layers per slice.

**Layer Allocation per Slice**. This experiment aims to answer the question: how many slices can we pack into a model while still achieving good performance? We conduct an experiment where we allocate different numbers of PEFT layers per slice and also vary the number of slices. We report the results on RTE dataset using RoBERTa<sub>LARGE</sub> in Figure 10. We observe that the performance is poor when the number of layers per slice is low. For example, when the number of layers per slice = 1, the performance improves as we increase the number of slices but again drops when the slice count is too high. This shows that it may not be feasible to train the model using a large number of slices without a drop in performance. Overall, the performance variation depends on the underlying task and model, so the developer should select these hyperparameters based on their performance requirements.

**Sequence-based Training**. In this experiment, we compare  $S^3T$ 's performance with sequential training. Sequential training involves training the entire PEFT model on a sequence of slices. This was used in [35] to improve the retraining efficiency of SISA. In Figure 11, we report the performance of  $S^3T$  and sequential training using  $ViT_{BASE}$  on CIFAR-10 and CIFAR-100 datasets. We observe that the performance of  $S^3T$  gradually increases as it is trained on more slices. Overall, we observe that  $S^3T$  achieves quite similar or outperforms sequential training. It is important to note that  $S^3T$  trains a significantly smaller number of parameters (L times reduction compared to sequential training) but still achieves competitive performance.

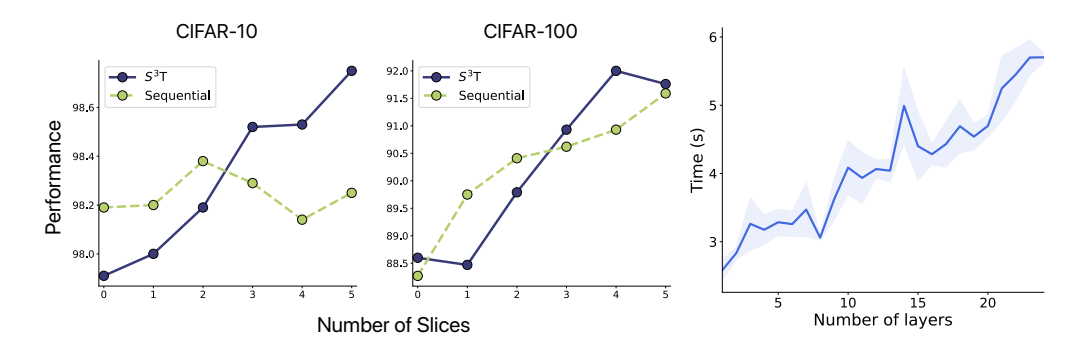


Figure 11: (*Left*) Comparison of sequential training with S<sup>3</sup>T using a PEFT model. We observe that S<sup>3</sup>T's performance gradually improves as it is trained on a larger number of slices, ultimately achieving similar performance to sequential training while being more efficient.

Table 3: Storage cost of S<sup>3</sup>T under different training budgets. We show how the deletion rate increases with an increased storage cost. The overall storage cost of PEFT layers is minimal and is equivalent to storing an additional model.

Budget	Model (GB)	PEFT (GB)	Del. Rate
B=1	1.2	0.21	66.4
B=2	1.2	0.42	86.9
B=3	1.2	0.63	100.8
B=4	1.2	0.84	107.8
B=5	1.2	1.05	110.1
B=6	1.2	1.26	124.1

**Training Time**. In this experiment, we evaluate the training time with a varying number of PEFT layers. In Figure 11 (right), we report the average training time over a constant number of steps using RoBERTa<sub>LARGE</sub> model. We observe that training time linearly increases as an increased number of LoRA layers are trained. This shows the effectiveness of our proposed S<sup>3</sup>T framework, which only trains a small number of PEFT layers at each training stage.

Storage Costs. In this experiment, we evaluate how the storage cost of  $S^3T$  grows with an increasing budget and its effect on the overall deletion rate. In Table 3, we report the storage costs and deletion rate of training ViT<sub>LARGE</sub> model with m=5 shards and L=6 slices per shard. We observe that the storage cost of PEFT layers (with LoRA rank=16) is considerably less compared to the full model size. As the budget and storage cost increases there is an improvement in the deletion rate. However, the rate of improvement of the deletion rate slows down with an increased budget, indicating there is a lesser return on increasing the budget.

## **D** Limitations

In this paper, we present a novel exact unlearning framework,  $S^3T$ .  $S^3T$  improves the deletion rate of existing unlearning systems at the cost of additional offline training. The training process can be time-consuming if we are fine-tuning larger models and have a higher performance requirement (thereby high budget B). However, this is an inherent tradeoff between offline training and losing revenue due to re-training costs. The developer should adjust their budget according to the tradeoff in their specific application.

# **E** Broader Impact

We present a scalable approach to perform exact unlearning in production systems. We hope that this framework will be adopted by organizations and enable a cost-effective way to ensure the privacy requests of various users. In general, unlearning systems are susceptible to attacks where the adversary may design deletion requests in a way to modify the model behaviour according to their needs. Therefore, it is important to ensure that the deletion requests executed on the unlearning system are not malicious. However, this is a limitation of unlearning systems in general and not specific to our proposed framework, S<sup>3</sup>T. Future works can focus on the identification of malicious unlearning requests.